Yan and Fang *EURASIP Journal on Wireless Communications and Networking* 2014, **2014**:127
http://jwcn.eurasipjournals.com/content/2014/1/127

EURASIP Journal on Wireless Communications and Networking
a SpringerOpen Journal

RESEARCH Open Access

Reliability evaluation of 5G C/U-plane decoupled architecture for high-speed railway

Li Yan*† and Xuming Fang†

Abstract

To facilitate the mobility of heterogeneous networks, control plane (C-plane) and user plane (U-plane) decoupled architecture is being considered by the fifth generation (5G) wireless communication network, in which relatively crucial C-plane is expanded and kept at dependable lower frequency bands to guarantee transmission reliability and the corresponding U-plane is moved to available higher frequency bands to boost capacity. Moreover, we apply this architecture to future professional high-speed railway wireless communication system to fulfill the wireless access desire of train passengers. However, for such emerging architecture, there still exist many problems to be solved to guarantee the reliable transmission. In this article, the problem of how to appropriately evaluate the transmission reliability of C/U-plane decoupled architecture is investigated. Due to the lack of ability to reflect the importance of C-plane, conventional outage probability cannot properly indicate the transmission reliability of C/U-plane decoupled architecture whose primary design consideration is that C-plane more heavily affects the transmission reliability thereby being kept at dependable lower frequency bands. Based on this, a novel indicator named unreliability factor (URF) is proposed. Theoretical analysis and simulation results demonstrate that URF can exactly highlight the effects of C-plane on the entire transmission process. Hence, it is more appropriate to employ URF as the indicator to evaluate the transmission reliability of C/U-plane decoupled architecture.

Keywords: 5G; C/U-plane decoupled architecture; Transmission reliability; Reliability evaluation; High-speed railway

Introduction

To cater to the exponentially increasing traffic volume requirements in public mobile network, higher frequency bands with wider spectrum are exploited to further extend the capacity of Long-Term Evolution (LTE) network. Unfortunately, compared with lower frequency bands, higher frequency bands suffer from severer propagation loss which seriously limits the coverage. Hence, cells working at higher frequency bands are called small cells. On the account of mobility performance, small cells are usually overlaid on the coverage of macro cells that use lower frequency bands, which forms heterogeneous network. However, as deployment gets increasingly dense, the huge redundant control signaling interaction caused by frequent handovers between small and macro cells reduces the efficiency of heterogeneous networks. In order to mitigate this situation, C/U-plane decoupled architecture is proposed for upcoming 5G wireless communication network [1,2]. In this architecture, the relatively important C-plane is extended and kept at lower frequency bands of macro cells. In addition, the main capacity demander U-plane is moved to the small cells using available higher frequency bands with wider spectrum. With considerable coverage of macro cells, much fewer handovers happen to the C-plane compared to conventional coupled architecture of heterogeneous networks. Therefore, under a macro cell, the handover process is just simplified to the U-plane handover, which saves lots of control signaling interaction.

With the remarkable success of railway industry and wireless technologies, train passengers are eager to enjoy the Internet during long-distance journey. However, existing narrowband GSM-R (Global System for Mobile Communication for Railway) which is originally designed to transmit low-volume train control information cannot afford this huge capacity. In order to provide broadband

*Correspondence: liyan12047001@my.swjtu.edu.cn
†Equal contributors
Institute of Mobile Communications, Southwest Jiaotong University, Chengdu 610031, China

services for train passengers, railway wireless communication system is confronting the evolution to its next generation. With enhanced robustness, LTE is the most potential one for the evolution [3,4]. Based on this, in our previous work [5,6], we applied C/U-plane decoupled architecture to future professional high-speed railway wireless communication system to fulfill the wireless access desire of train passengers and the network architecture is depicted in Figure 1. With consideration of the return on investment, no public mobile network operator would like to offer a thorough coverage for most sparsely populated railway scenarios. Nevertheless, in the C/U-plane decoupled railway wireless network, both train control information and passengers' services can be transmitted. This provides a better choice for passengers to get a higher-quality service. Furthermore, on account of the severe challenges faced by high-speed railway scenario such as large penetration loss and group handover, it is difficult for passengers inside the train to hold a dependable connection with outside base station directly. Hence, as shown in Figure 1, mobile relay (MR) and access point (AP), which are connected with each other via optical fiber, are separately mounted on the roofs outside and inside the train [7]. This also provides a potential way to save operators' infrastructure cost by converging different air interface technologies (e.g., LTE/3G/2G/Wi-Fi) on the AP and employing LTE on the link between MR and the outside base stations. Inside the train, passengers connect to the AP and then their data are forwarded to outside base stations via MR. In the C/U-plane decoupled architecture, C-plane signaling and U-plane data of train passengers' services are separately transmitted by the macro and small cells. The macro cell employs lower frequency bands to provide good connectivity and mobility of C-plane and the small cell works at available higher frequency bands to expand capacity. On account of transmission reliability, crucial train control information is entirely kept at lower frequency bands without decoupling. As a result, train control information and data of passengers are separately transmitted through different nodes. In this way, the artificial interference from the passengers is avoided, thereby enhancing the security to some extent. However, this is already out of the scope of our study. In addition, this article focuses on the effect of decoupled C/U-plane on the transmission reliability of passengers' services.

For clarity, the booming LTE network is employed as the benchmark system for following analysis. In LTE network, C-plane is responsible for essential control operations such as broadcasting system information, network attaches, paging ,and mobility management [8]. Moreover, the functionality of U-plane is to forward user data flow. Definitely, without a reliable C-plane, the U-plane cannot work properly. From the perspective of air interfaces, without reliably transmitted Physical Downlink Control Channel (PDCCH) that accommodates control information to indicate 'who' the data are for, 'what' data are sent, and 'how' the data are sent on Physical Downlink Shared Channel (PDSCH), the user data cannot be correctly decoded. Considering the above mentioned in [9,10], the crucial C-plane instead of U-plane is kept at dependable lower frequency bands so that the transmission reliability of C/U-plane decoupled architecture could be well guaranteed. However, the performance evaluation of this architecture has not been well studied. Actually, for such emerging network architecture, there still exist many problems to be solved to guarantee the reliable transmission. For instance, Doppler effect is always a severe challenge for high-speed railway

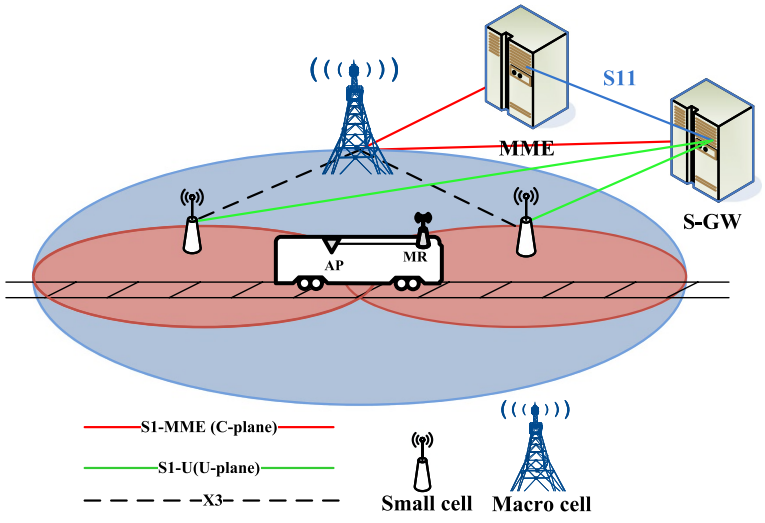

Figure 1 C/U-plane decoupled architecture in high-speed railway.

scenario. While in the C/U-plane decoupled architecture, C-plane and U-plane of the same user are transmitted at different frequencies thereby facing different Doppler shifts and Doppler spreads. Hence, the Doppler effect may get even worse. Fortunately, railways are mostly built in wide suburban or viaduct environment where multipaths can be neglected and the wireless channel can be regarded as LOS [4]. Thus, there almost exists no Doppler spread in high-speed railway scenario. According to [4,6], with a known train's location and velocity supplied by the communication-based train control (CBTC) system, it can be assumed that Doppler shifts are separately compensated for C-plane and U-plane. Hence, how to appropriately evaluate the transmission reliability of this decoupled architecture becomes an urgent problem, which will greatly impact subsequent research directions on performance enhancement.

In wireless networks, the outage probability defined as the probability that the received signal quality is lower than some threshold is a popularly used indicator to reflect the transmission reliability [11,12]. Under this definition, the outage probability of C/U-plane decoupled architecture can be expressed as the complementary probability of an event that both signal qualities of C-plane and U-plane are larger than the outage threshold. Obviously, from the view of air interface reliability, the effects of C-plane and U-plane on outage probability are virtually equal. That is to say, due to the lack of ability to reflect the importance of C-plane, the conventional outage probability cannot properly indicate the transmission reliability of C/U-plane decoupled architecture whose primary design consideration is that C-plane more heavily affects the transmission reliability thereby being kept at dependable lower frequency bands.

To facilitate the presentation, except for special behaviors such as paging and handover, we only take the general communication process as an example to qualitatively analyze the reliability relationship between C-plane and U-plane. In terms of theoretical analysis based on signal quality of air interface, the analysis procedures and results of uplink and downlink are the same. Hence, for simplicity, the following analysis is just on the basis of downlink. In the general communication process of C/U-plane decoupled architecture, PDSCH served by the small cell carries user date and PDCCH provided by the macro transmits corresponding control information such as transmission format to help receiver correctly decode the data on PDSCH. For PDCCH, its symbol error rate (SER) is directly caused by its poorly received signal quality. Nevertheless, these errors of PDCCH will badly affect the decoding correctness of data on PDSCH [13]. As a consequence for PDSCH, its errors result from two aspects, some of which are caused by its own poor signal quality and others are induced from the errors of PDCCH. In practice, if SER of PDCCH exceeds some threshold, then no matter how well the signal quality of PDSCH is, the receiver cannot correctly decode the data on PDSCH. Based on this, a more appropriate indicator named unreliability factor (URF) which can highlight the importance of C-plane is proposed to evaluate the transmission reliability of C/U-plane decoupled architecture.

The rest of this article is arranged as follows. 'Radio propagation model' section gives the propagation model for C/U-plane decoupled architecture. 'System outage probability of C/U-plane decoupled architecture' section proves that conventional outage probability cannot properly indicate the transmission reliability of this architecture. 'System reliability-based reliability evaluation method' section describes the proposed indicator URF and its appropriateness in evaluating the transmission reliability of this architecture. Finally, 'Conclusions' section concludes the whole article.

Radio propagation model

SIR model

Since the communication system in high-speed railway scenario has a linear topology, the macro and small cells of C/U-plane decoupled architecture are deployed on a straight line with vertical distance of D to the rail as shown in Figure 2. Suppose the base stations' radiation is omnidirectional, and the coverage radiuses of macro and small cell are R_{C} and R_{U} respectively. Besides, the abscissa axis coinciding with the driving direction is set to facilitate the expression of train travel distance d. Without loss of generality, two macro cells are considered in the following analysis, i.e., the analysis scope of d is from 0 to $4R_{\mathrm{C}}$-$2a_{\mathrm{C}}$, where a_{C} is the overlapping area distance of two macro cells and as shown in Figure 2, the overlapping area distance of two small cells is denoted by a_{U}.

Suppose the train starts from the origin and travels through distance of d, then the C-plane signal propagation distance between the train and macro cell is

$$x_{\mathrm{C}}(d)=\sqrt{\left(d-\left\lfloor\frac{d}{2R_{\mathrm{C}}-a_{\mathrm{C}}}\right\rfloor\cdot(2R_{\mathrm{C}}-a_{\mathrm{C}})-\left(R_{\mathrm{C}}-\frac{a_{\mathrm{C}}}{2}\right)\right)^2+D^2} \tag{1}$$

where $\lfloor\cdot\rfloor$ denotes rounding down operation.

Correspondingly, the U-plane signal propagation distance between the train and current serving small cell can be expressed as

$$x_{\mathrm{U}}(d)=\sqrt{\left(d-\left\lfloor\frac{d}{2R_{\mathrm{U}}-a_{\mathrm{U}}}\right\rfloor\cdot(2R_{\mathrm{U}}-a_{\mathrm{U}})-\left(R_{\mathrm{U}}-\frac{a_{\mathrm{U}}}{2}\right)\right)^2+D^2} \tag{2}$$

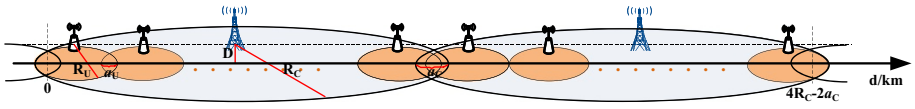

Figure 2 Geometric sketch for analysis.

Generally, the propagation attenuation is modeled as the product of path loss and a log-normal component representing shadow fading [14]. Then, with transmit power of P_t, the received signal-to-interference ratio (SIR) can be expressed as

$$\mathrm{SIR}(x) = \frac{P_t \cdot \mathrm{PL}(x) \times 10^{-\varepsilon/10}}{I} \tag{3}$$

where $\mathrm{PL}(x)$ is the path loss with propagation distance of x; ε is the decibel attenuation due to shadow fading with zero mean and standard variance σ; and the co-channel interference I is given by

$$I = \sum_{n=1}^{N_{\mathrm{eNB}}} P_t \cdot \mathrm{PL}(x_n) \tag{4}$$

where N_{eNB} represents the number of co-channel eNodeBs.

Consequently, the received signal quality of C-plane and U-plane can be separately computed as

$$\mathrm{SIR_C}(x_C(d)) = \frac{P_{t,C} \cdot \mathrm{PL_C}(x_C(d)) \times 10^{-\varepsilon_C/10}}{I_C} \tag{5}$$

$$\mathrm{SIR_U}(x_U(d)) = \frac{P_{t,U} \cdot \mathrm{PL_U}(x_U(d)) \times 10^{-\varepsilon_U/10}}{I_U} \tag{6}$$

For clarity, subscripts of parameters that relate to C-plane are set to C. And for U-plane they are set to U. However, in fact P_t, $\mathrm{PL}(x)$, ε, and I are determined by current serving base station while not the plane, that is, $P_{t,C}$, $\mathrm{PL_C}(x)$, ε_C and I_C are the properties of the macro cell which serves the C-plane. With subscript U, they are the properties of the small cell which provides U-plane. The above also applies to the following expressions.

Cross-correlated shadow fading

Shadow fading is a large-scale phenomenon which depends on the surrounding communication environment. Although in C/U-plane decoupled architecture the macro and small cell are deployed at different locations, they simultaneously serve the same train user. Hence, there exist some common components between the propagation paths of macro cell and small cell signals, especially for the area near the train. As a consequence, the shadow fading of macro and small cells are cross-correlated. Based on [15,16], cross-correlation of shadow fading can be explained by a partial overlap of the large-scale propagation medium as shown in Figure 3, and non-overlapping propagation areas are considered independent.

Then, the shadow fading can be decomposed as

$$\begin{aligned} \varepsilon_C &= W + W_C \\ \varepsilon_U &= W + W_U \end{aligned} \tag{7}$$

where W, W_C, and W_U are independent Gaussian random variables with zero mean and standard variances a, b, and c, respectively, and they satisfy

$$\begin{aligned} {\sigma_C}^2 &= a^2 + b^2 \\ {\sigma_U}^2 &= a^2 + c^2 \\ E[\varepsilon_C \varepsilon_U] &= a^2 = \rho_{C,U}\sigma_C\sigma_U \end{aligned} \tag{8}$$

According to [13], the cross-correlation coefficient of shadow fading can be modeled as

$$\rho_{C,U}(d) = \rho_{U,C}(d) = \begin{cases} \sqrt{\frac{\min(x_C(d),x_U(d)))}{\max(x_C(d),x_U(d))}}, & 0 \le \Theta \le \Theta^{\mathrm{T}} \\ \left(\frac{\Theta^T}{\Theta}\right)^{\gamma} \sqrt{\frac{\min(x_C(d),x_U(d))}{\max(x_C(d),x_U(d))}}, & \Theta^{\mathrm{T}} \le \Theta \le \pi \end{cases} \tag{9}$$

where γ is referred to as a parameter determined by the size and height of terrain and the height of base station and is generally set to 0.3 [17]; Θ^{T} corresponds to the angle threshold that depends on the serial de-correlation distance d_{cor} and is defined as

$$\Theta^{\mathrm{T}} = 2\arctan\left(\frac{d_{\mathrm{cor}}}{2\min\left(x_C(d), x_U(d)\right)}\right) \tag{10}$$

Moreover, Θ of (9) is the angle between the propagation paths of C-plane and U-plane signals as shown in Figure 3. As the site-to-site distance between macro and small cells can be calculated via the following equation

$$x_{\mathrm{sep}}(d) = \begin{cases} (2R_U - a_U) \cdot \left(\left\lfloor \frac{\sqrt{{x_C}^2(d) - D^2}}{2R_U - a_U} \right\rfloor - \frac{1}{2} \right), d = 0, d = 4R_C - 2a_C \\ (2R_U - a_U) \cdot \left(\left\lfloor \frac{\sqrt{{x_C}^2(d) - D^2}}{2R_U - a_U} \right\rfloor + \frac{1}{2} \right), \text{otherwise} \end{cases} \tag{11}$$

the included angle Θ can be derived as

$$\Theta(d) = \arccos\left(\frac{{x_C}^2(d) + {x_U}^2(d) - {x_{\mathrm{sep}}}^2(d)}{2x_C(d)x_U(d)}\right) \tag{12}$$

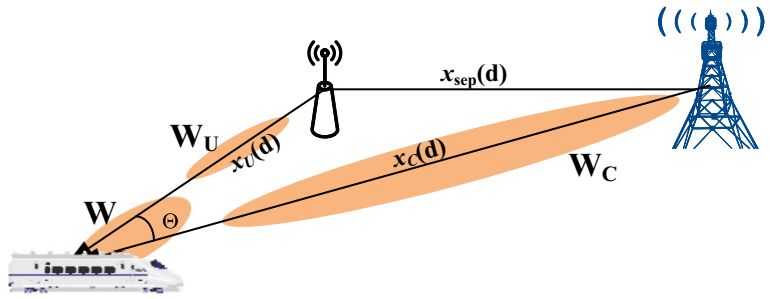

Figure 3 Cross-correlated shadow fading.

Then, substitute (12) into (9), $\rho_{(C,U)}$ is obtained, with which the standard variances, $a(d)$, $b(d)$, and $C(d)$ in (8) can be worked out.

System outage probability of C/U-plane decoupled architecture

Generally, outage probability is used to evaluate transmission reliability of wireless communication networks. It is defined as the probability that the received SIR is lower than some threshold. Based on this, the system outage probability of C/U-plane decoupled architecture can be derived as

$$\begin{aligned}
P_{\text{out,cov}} &= 1 - P\left[\text{SIR}_\text{C} > \text{SIR}_\text{C}^{\text{th}}, \text{SIR}_\text{U} > \text{SIR}_\text{U}^{\text{th}}\right] \\
&= 1 - P\left[10\lg\frac{P_{\text{t,C}}\cdot\text{PL}_\text{C}(x_\text{C}(d))}{I_\text{C}} - W - W_\text{C} > \text{SIR}_\text{C}^{\text{th}},\right. \\
&\quad \left. 10\lg\frac{P_{\text{t,U}}\cdot\text{PL}_\text{U}(x_\text{U}(d))}{I_\text{U}} - W - W_\text{U} > \text{SIR}_\text{U}^{\text{th}}\right] \\
&= 1 - \frac{1}{\left(\sqrt{2\pi}\right)^3 a(d)b(d)c(d)}\int_{-\infty}^{+\infty} e^{-\frac{W^2}{2a^2(d)}} \\
&\quad \times \left(\int_{-\infty}^{10\lg\frac{P_{\text{t,C}}\cdot\text{PL}_\text{C}(x_\text{C}(d))}{I_\text{C}} - W - \text{SIR}_\text{C}^{\text{th}}} e^{-\frac{W_\text{C}^2}{2b^2(d)}} dW_\text{C}\right. \\
&\quad \left.\int_{-\infty}^{10\lg\frac{P_{\text{t,U}}\cdot\text{PL}_\text{U}(x_\text{U}(d))}{I_\text{U}} - W - \text{SIR}_\text{U}^{\text{th}}} e^{-\frac{W_\text{U}^2}{2c^2(d)}} dW_\text{U}\right) dW \\
&= 1 - \frac{1}{\sqrt{2\pi}}\int_{-\infty}^{+\infty} e^{-\frac{t^2}{2}}\Phi \\
&\quad \times \left(\frac{10\lg\frac{P_{t,C}\cdot\text{PL}_\text{C}(x_\text{C}(d))}{I_\text{C}} - a(d)t - \text{SIR}_\text{C}^{\text{th}}}{b(d)}\right) \\
&\quad \times \Phi\left(\frac{10\lg\frac{P_{\text{t,U}}\cdot\text{PL}_\text{U}(x_\text{U}(d))}{I_\text{U}} - a(d)t - \text{SIR}_\text{U}^{\text{th}}}{c(d)}\right) dt
\end{aligned} \tag{13}$$

where $\text{SIR}_\text{C}^{\text{th}}$ and $\text{SIR}_\text{U}^{\text{th}}$ are the decibel outage thresholds of C-plane and U-plane, respectively, and

$$\Phi(x) = \frac{1}{\sqrt{2\pi}}\int_{-\infty}^{x} e^{-\frac{t^2}{2}} dt \tag{14}$$

Considering the fairness of comparison, outage probabilities of coupled macro and small cell architectures are also computed as the complementary probability of an event that both the signal qualities of C-plane and U-plane are larger than the outage thresholds, that is,

$$\begin{aligned}
P_{\text{out,m}} &= 1 - \int_{-\infty}^{+\infty} \frac{e^{-\frac{t^2}{2}}}{\sqrt{2\pi}}\Phi \\
&\quad \times \left(\frac{10\lg\frac{P_{\text{t,C}}\cdot\text{PL}_\text{C}(x_\text{C}(d))}{I_\text{C}} - a(d)t - \text{SIR}_\text{C}^{\text{th}}}{b(d)}\right)^2 dt
\end{aligned} \tag{15}$$

$$\begin{aligned}
P_{\text{out,s}} &= 1 - \int_{-\infty}^{+\infty} \frac{e^{-\frac{t^2}{2}}}{\sqrt{2\pi}}\Phi \\
&\quad \times \left(\frac{10\lg\frac{P_{\text{t,U}}\cdot\text{PL}_\text{U}(x_\text{U}(d))}{I_\text{U}} - a(d)t - \text{SIR}_\text{U}^{\text{th}}}{c(d)}\right)^2 dt
\end{aligned} \tag{16}$$

Based on the above modeling, a numerical simulation is conducted and the results are shown in Figures 4 and 5, where Figure 4 depicts the outage probabilities of different network architectures and Figure 5 corresponds to the trend in Figure 4. Detailed simulation parameters are listed in Table 1.

From the above theoretical analysis and simulation, it is easy to find that in terms of the air interface reliability, the effects of C-plane and U-plane on outage probability are virtually equal. As shown in Figures 4 and 5, the transmission performance of C/U-plane decoupled

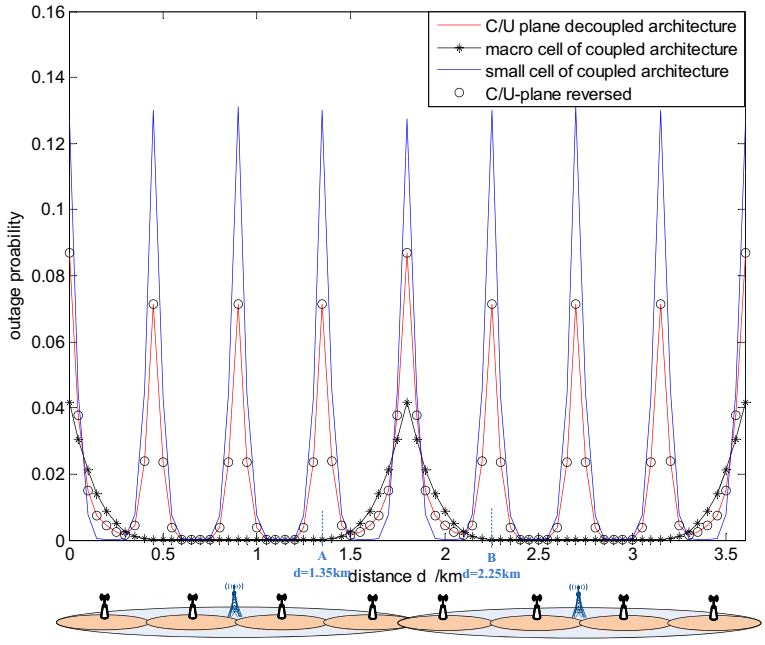

Figure 4 Reliability evaluation under conventional outage probability.

architecture is just the averaging of that of coupled macro cell and small cell architectures. For instance, at the scope (A, B), although C-plane cannot be reliably transmitted, the entire system performance of C/U-plane decoupled architecture is not so poor. While at the center of macro cell, no matter how reliably C-plane performs, the entire transmission reliability of C/U-plane decoupled architecture is badly affected by the poor U-plane. Besides, if C-plane and U-plane are reversed, i.e., U-plane is kept at macro cell and C-plane is moved to small cell, the result of outage probability has not changed. This thoroughly reveals that the conventional system outage probability

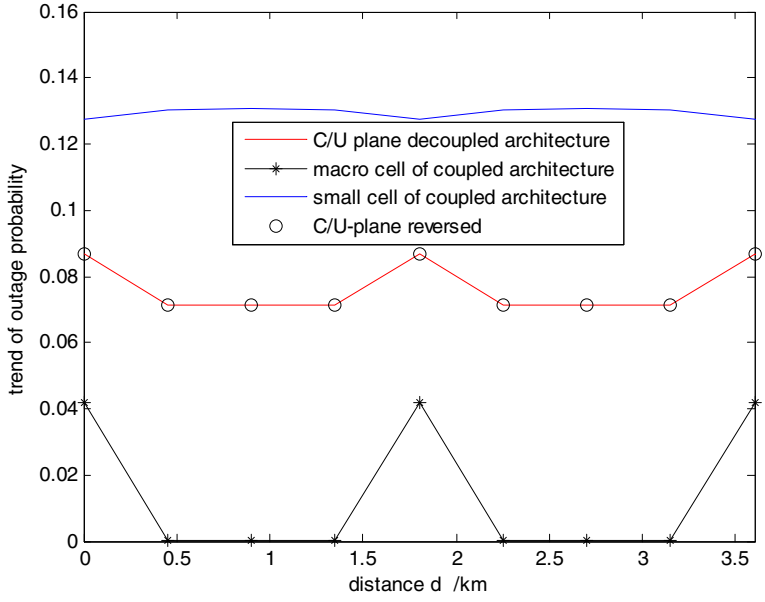

Figure 5 Trends of outage probability in Figure 4.

Table 1 Simulation parameters [18]

Parameters	Values
Frequency of macro cell	2 GHz
Frequency of small cell	5 GHz
Path loss model of macro cell PL_C	Hata
Path loss model of small cell PL_U	M.2135
Transmit power of macro cell $P_{t,C}$	43 dBm
Transmit power of small cell $P_{t,U}$	33 dBm
Radius of macro cell R_C	1 km
Radius of small cell R_U	0.25 km
Overlapping area distance of macro cells a_C	0.2 km
Overlapping area distance of small cells a_U	0.05 km
Distance between base station and rail D	30 m
C-plane SER threshold th_C	10^{-6}
U-plane SER threshold th_U	10^{-2}
$\alpha(th_C)$	10^{-4}
Correlation distance d_{cor}	100 m [19]
Modulation scheme of U-plane	16QAM
Standard variance of C-plane shadowing σ_C	6 dB
Standard variance of U-plane shadowing σ_U	8 dB

cannot convey the primary design consideration of C/U-plane decoupled architecture that C-plane more heavily affects transmission reliability than U-plane thereby being kept at dependable lower frequency bands. Hence, it is not proper to employ simple outage probability as the indicator to evaluate the transmission reliability of this decoupled architecture.

System reliability-based reliability evaluation method

Reliability relationship between C-plane and U-plane

As mentioned before, in the general communication process, PDSCH served by the small cell carries user data, and the corresponding PDCCH served by the macro cell transmits control information such as modulation and coding scheme of PDSCH to help the receiver correctly decode the data on PDSCH. For PDCCH, its transmission errors are just caused by its poor SIR_C. However, for PDSCH there are two aspects resulting in data errors. As shown in Figure 6, some errors of PDSCH are due to the poor received signal quality, while others are induced from the errors of PDCCH. Maybe, these parts of symbols are of high signal quality, but they cannot be correctly decoded because of the inaccurate transmission format indication on PDCCH. Hence, it is reasonable to believe that if SER of PDCCH exceeds some tolerable value, then no matter how well the signal quality of PDSCH is, the data cannot be correctly received. This exactly reveals why C-plane is regarded more crucial than U-plane. Although how the errors of PDCCH affects the data receiving on PDSCH is beyond the scope of this study, a mapping function is required to describe the relationship between SERC and SERU/C that is

$$\mathrm{SER_{U/C}} = \alpha\,(\mathrm{SER_C}) \tag{17}$$

where α function is supposed to be monotone increasing with definition field of SER_C from 0 to 1 and range of $SER_{U/C}$ from 0 to 1 as well. However, the exact expression of α function depends on the system settings and is out of our study scope.

Unreliability factor

Through the above discussion, it can be concluded that for C/U-plane decoupled architecture, a proper indicator is needed that can exactly highlight the importance of C-plane. Based on this, a novel indicator named unreliability factor, URF, is proposed to appropriately evaluate the system transmission reliability of C/U-plane decoupled architecture, which is defined as

$$\mathrm{URF} = \begin{cases} P(\mathrm{SER_U} > \mathrm{th_U}), & \mathrm{SER_C} \le \mathrm{th_C} \\ 1, & \mathrm{SER_C} > \mathrm{th_C} \end{cases} \tag{18}$$

It is obvious that URF has the ability to reflect the importance of C-plane. When the SER of crucial C-plane is beyond the threshold th_C, in spite of the transmission performance of PDSCH, URF is directly set to 1. This exactly conforms to the previous analysis result that if SER of PDCCH exceeds some tolerable value, then no matter how well the signal quality of PDSCH is, the data cannot be correctly received. While if C-plane is reliably transmitted, the value of URF will depend on the SER outage probability of PDSCH which is defined as the probability that the SER is higher than some threshold [20]. Practically, the SER outage probability of PDSCH is much lower than 1. Hence, at the point of $SER_C = th_C$, URF is not rightly continuous thereby not a probability function. As a matter of fact, URF can be interpreted as a kind of indicator, which equals to a complex and reasonable probability value.

From the SIR modeling in 'Radio propagation model' section, it can be found that due to the cross-correlation of shadow fading between the macro and small cells, SIR_C and SIR_U are not absolutely independent. Then, it seems that $SER_{U/C}$ and SER_{U/SIR_U} are correlated. Fortunately, there exists the principle of conditional independence that two random variables X and Y are conditionally indepen-

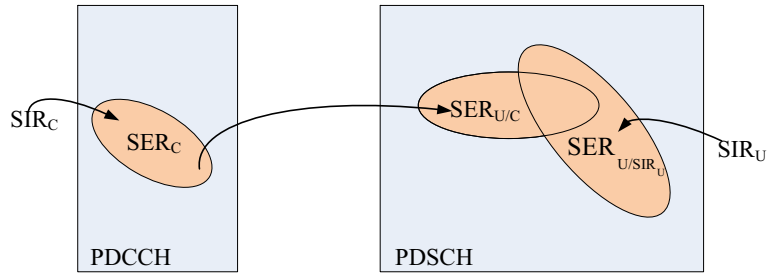

Figure 6 Reliability relationship between C-plane and U-plane.

dent if given Z as shown in Figure 7 [21], that is, with given Z, for any real number x, y, and z, the following equation is satisfied:

$$P_{X,Y/Z}(x, y/z) = P_{X/Z}(x/z)\, P_{Y/Z}(y/z) \tag{19}$$

Based on this, since the relationship between $\mathrm{SIR_C}$ and $\mathrm{SER_C}$ is known, $\mathrm{SIR_C}$ and $\mathrm{SER_{U/C}}$ are conditionally independent. Therefore, $\mathrm{SER_{U/C}}$ and $\mathrm{SER_{U/SIR_U}}$ are conditionally independent and the total SER of U-plane can be derived as

$$\mathrm{SER_U} = \mathrm{SER_{U/C}} + \mathrm{SER_{U/SIR_U}} - \mathrm{SER_{U/C}} \cdot \mathrm{SER_{U/SIR_U}} \tag{20}$$

In LTE network, the modulation scheme for C-plane is QPSK, and its SER can be expressed as [22]

$$\mathrm{SER_C} = 2Q\left(\sqrt{2\mathrm{SIR_C}}\right)\left(1 - \frac{1}{2}Q\left(\sqrt{2\mathrm{SIR_C}}\right)\right) \tag{21}$$

where Q function is defined by

$$Q(x) = \frac{1}{\sqrt{2\pi}} \int_x^{\infty} e^{-\frac{t^2}{2}} dt \tag{22}$$

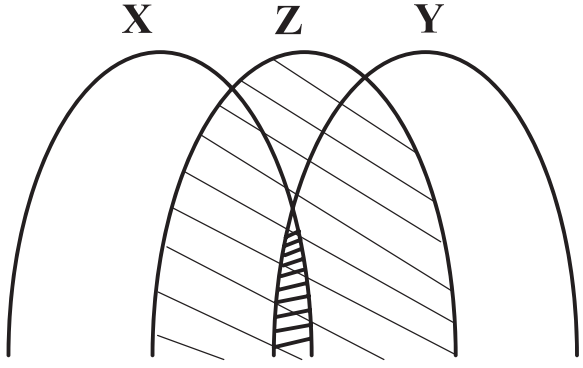

Figure 7 Conditional independence.

Then, the transition condition in the definition of URF can be further derived as

$$\begin{aligned} & 2Q\left(\sqrt{2\mathrm{SIR_C}}\right)\left(1 - \frac{1}{2}Q\left(\sqrt{2\mathrm{SIR_C}}\right)\right) \le \mathrm{th_C} \\ & \Rightarrow \mathrm{SIR_C} \ge \frac{\left(Q^{-1}\left(1 - \sqrt{1 - \mathrm{th_C}}\right)\right)^2}{2} \\ & \Rightarrow \varepsilon_{\mathrm{C}} \le -10 \lg\left(\frac{I_{\mathrm{C}}\left(Q^{-1}\left(1 - \sqrt{1 - \mathrm{th_C}}\right)\right)^2}{2P_{\mathrm{t,C}}\mathrm{PL_C}(x_{\mathrm{C}}(d))}\right) = C\left(x_{\mathrm{C}}(d)\right) \end{aligned} \tag{23}$$

where Q^{-1} is the inverse function of Q function, and $C(x_{\mathrm{C}}(d))$ is defined to simplify the following expressions.

For U-plane with modulation scheme of M-QAM, $\mathrm{SER_{U/SIR_U}}$ is given by [22]

$$\mathrm{SER_{U/SIR_U}} = 4\left(1 - \frac{1}{\sqrt{M}}\right) Q\left(\sqrt{\frac{3\log_2 M}{M-1}\mathrm{SIR_U}}\right) \tag{24}$$

Then, the SER outage probability of U-plane in the definition of URF can be further derived as

$$\begin{aligned} & \mathrm{SER_{U/C}} + \mathrm{SER_{U/SIR_U}} - \mathrm{SER_{U/C}} \cdot \mathrm{SER_{U/SIR_U}} \ge \mathrm{th_U} \\ & \Rightarrow \alpha(\mathrm{SER_C}) + (1 - \alpha(\mathrm{SER_C}))\,\mathrm{SER_{U/SIR_U}} \ge \mathrm{th_U} \\ & \Rightarrow \mathrm{SER_{U/SIR_U}} \ge \frac{\mathrm{th_U} - \alpha(\mathrm{SER_C})}{1 - \alpha(\mathrm{SER_C})} = \frac{\mathrm{th_U} - 1}{1 - \alpha(\mathrm{SER_C})} + 1 \end{aligned} \tag{25}$$

As in practice , $\mathrm{th_U} < 1$, then

$$\frac{\mathrm{th_U} - 1}{1 - \alpha(\mathrm{SER_C})} + 1 \ge \frac{\mathrm{th_U} - 1}{1 - \alpha(\mathrm{th_C})} + 1 = \frac{\mathrm{th_U} - \alpha(\mathrm{th_C})}{1 - \alpha(\mathrm{th_C})} \tag{26}$$

Under more stringent condition, $\mathrm{SER}_{\mathrm{U/SIR_U}}$ of (19) can be further expressed as

$$\begin{aligned}
&\mathrm{SER}_{\mathrm{U/SIR_U}} \geq \frac{\mathrm{th_U} - \alpha\left(\mathrm{th_C}\right)}{1-\alpha\left(\mathrm{th_C}\right)} \\
&\Rightarrow 4\left(1-\frac{1}{\sqrt{M}}\right) Q\left(\sqrt{\frac{3\log_2 M}{M-1}\mathrm{SIR_U}}\right) \geq \frac{\mathrm{th_U} - \alpha\left(\mathrm{th_C}\right)}{1-\alpha\left(\mathrm{th_C}\right)} \\
&\Rightarrow \mathrm{SIR_U} \leq \frac{(M-1)}{3\log_2 M}\left(Q^{-1}\left(\frac{\mathrm{th_U} - \alpha\left(\mathrm{th_C}\right)}{4\left(1-\frac{1}{\sqrt{M}}\right)\left(1-\alpha\left(\mathrm{th_C}\right)\right)}\right)\right)^2 \\
&\Rightarrow \varepsilon_{\mathrm{U}} \geq -10\lg\left(\frac{I_{\mathrm{U}}(M-1)}{3\log_2 M \cdot P_{t,U}\cdot \mathrm{PL_U}(x_{\mathrm{U}}(d))}\right. \\
&\qquad \left.\times\left(Q^{-1}\left(\frac{\mathrm{th_U} - \alpha\left(\mathrm{th_C}\right)}{4\left(1-\frac{1}{\sqrt{M}}\right)\left(1-\alpha\left(\mathrm{th_C}\right)\right)}\right)\right)^2\right) \\
&\Rightarrow \varepsilon_{\mathrm{U}} \geq U(x_{\mathrm{U}}(d))
\end{aligned} \tag{27}$$

where $U\left(x_{\mathrm{U}}(d)\right)$ is defined to simplify the following expressions.

Hence, the definition of URF in (18) can be rewritten as

$$\mathrm{URF} = \begin{cases} P\left(W_{\mathrm{U}} > U\left(x_{\mathrm{U}}(d)\right) - W\right), & W_{\mathrm{C}} \leq C\left(x_{\mathrm{C}}(d)\right) - W \\ 1, & W_{\mathrm{C}} > C\left(x_{\mathrm{C}}(d)\right) - W \end{cases} \tag{28}$$

Then, the average URF can be obtained as

$$\begin{aligned}
\mathrm{URF}^{\mathrm{ave}} &= \frac{1}{\left(\sqrt{2\pi}\right)^3 a(d)b(d)c(d)}\int_{-\infty}^{+\infty} e^{-\frac{W^2}{2a^2(d)}} \\
&\quad\times\left(\int_{-\infty}^{C(x_{\mathrm{C}}(d))-W} P\left(W_{\mathrm{U}} > U\left(x_{\mathrm{U}}(d)\right) - W\right)\right. \\
&\quad\left.\times\, e^{-\frac{{W_{\mathrm{C}}}^2}{2b^2(d)}} dW_{\mathrm{C}} + \int_{C(x_{\mathrm{C}}(d))-W}^{\infty} e^{-\frac{{W_{\mathrm{C}}}^2}{2b^2(d)}} dW_{\mathrm{C}}\right) dW \\
&= \frac{1}{\sqrt{2\pi}a(d)}\int_{-\infty}^{+\infty} e^{-\frac{W^2}{2a^2(d)}}\left(Q\left(\frac{U\left(x_{\mathrm{U}}(d)\right) - W}{c(d)}\right)\right. \\
&\quad\left.\times\Phi\left(\frac{C\left(x_{\mathrm{C}}(d)\right)-W}{b(d)}\right) + Q\left(\frac{C\left(x_{\mathrm{C}}(d)\right)-W}{b(d)}\right)\right) dW
\end{aligned} \tag{29}$$

Under the proposed indicator, the average URF of coupled macro cell network architecture can be presented as

$$\begin{aligned}
\mathrm{URF_m}^{\mathrm{ave}} &= \frac{1}{\sqrt{2\pi}a(d)}\int_{-\infty}^{+\infty} e^{-\frac{W^2}{2a^2(d)}}\left(Q\left(\frac{U_{\mathrm{C}}\left(x_{\mathrm{C}}(d)\right)-W}{b(d)}\right)\right. \\
&\quad\left.\times\Phi\left(\frac{C_{\mathrm{C}}(x_{\mathrm{C}}(d))-W}{b(d)}\right) + Q\left(\frac{C_{\mathrm{C}}(x_{\mathrm{C}}(d))-W}{b(d)}\right)\right) dW
\end{aligned} \tag{30}$$

where

$$\begin{aligned}
U_{\mathrm{C}}(x_{\mathrm{C}}(d)) &= -10\lg\left(\frac{I_{\mathrm{C}}(M-1)}{3\log_2 M \cdot P_{\mathrm{t,C}}\cdot \mathrm{PL_C}(x_{\mathrm{C}}(d))}\right. \\
&\quad\left.\times\left(Q^{-1}\left(\frac{\mathrm{th_U} - \alpha\left(\mathrm{th_C}\right)}{4\left(1-\frac{1}{\sqrt{M}}\right)\left(1-\alpha\left(\mathrm{th_C}\right)\right)}\right)\right)^2\right) \\
&\quad\times C_{\mathrm{C}}(x_{\mathrm{C}}(d)) = -10\lg\left(\frac{I_{\mathrm{C}}\left(Q^{-1}\left(1-\sqrt{1-th_{\mathrm{C}}}\right)\right)^2}{2P_{\mathrm{t,C}}\mathrm{PL_C}(x_{\mathrm{C}}(d))}\right)
\end{aligned} \tag{31}$$

And for coupled small cell network architecture, the average URF is

$$\begin{aligned}
\mathrm{URF_s}^{\mathrm{ave}} &= \frac{1}{\sqrt{2\pi}a(d)}\int_{-\infty}^{+\infty} e^{-\frac{W^2}{2a^2(d)}}\left(Q\left(\frac{U_{\mathrm{U}}\left(x_{\mathrm{U}}(d)\right)-W}{c(d)}\right)\right. \\
&\quad\left.\times\Phi\left(\frac{C_{\mathrm{U}}(x_{\mathrm{U}}(d))-W}{c(d)}\right) + Q\left(\frac{C_{\mathrm{U}}(x_{\mathrm{U}}(d))-W}{c(d)}\right)\right) dW
\end{aligned} \tag{32}$$

where

$$\begin{aligned}
U_{\mathrm{U}}\left(x_{\mathrm{U}}(d)\right) &= -10\lg\left(\frac{I_{\mathrm{U}}(M-1)}{3\log_2 M \cdot P_{\mathrm{t,U}}\cdot \mathrm{PL_U}(x_{\mathrm{U}}(d))}\right. \\
&\quad\left.\times\left(Q^{-1}\left(\frac{\mathrm{th_U} - \alpha\left(\mathrm{th_C}\right)}{4\left(1-\frac{1}{\sqrt{M}}\right)\left(1-\alpha\left(\mathrm{th_C}\right)\right)}\right)\right)^2\right) \\
C_{\mathrm{U}}\left(x_{\mathrm{U}}(d)\right) &= -10\lg\left(\frac{I_{\mathrm{U}}\left(Q^{-1}\left(1-\sqrt{1-\mathrm{th_C}}\right)\right)^2}{2P_{\mathrm{t,U}}\mathrm{PL_U}(x_{\mathrm{U}}(d))}\right)
\end{aligned} \tag{33}$$

On the basis of above theoretical analysis, numerical simulation is performed as shown in Figures 8 and 9. The simulation parameters are set as in Table 1. From Figure 8, at the scope (A, B), the entire performance of C/U-plane decoupled architecture is badly degraded by the poor transmission of C-plane, which just like that of

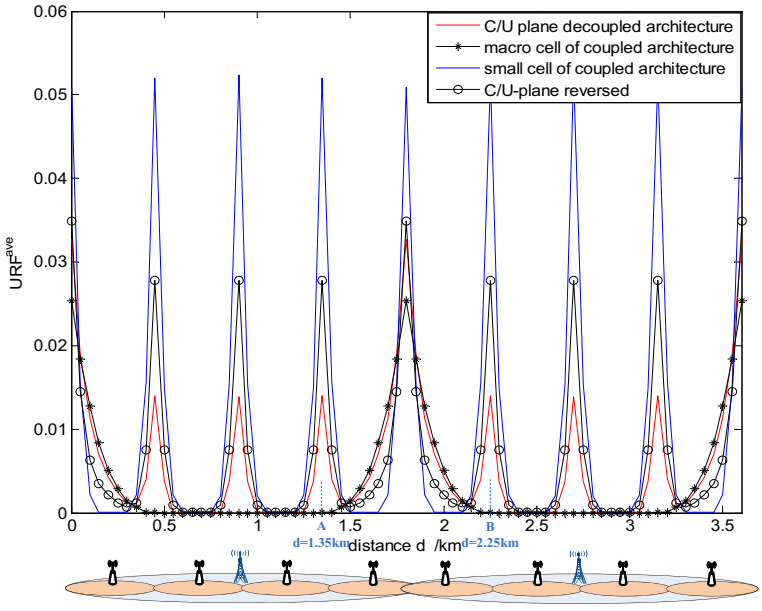

Figure 8 URF^{ave} of different network architectures.

coupled macro cell architecture. While at the center of macro cell, thanks to the well-transmitted C-plane, the entire performance of C/U-plane decoupled architecture is not so badly affected by the poor U-plane. Besides, for the reversed case that C-plane is moved to small cell and U-plane is kept at macro cell, the entire performance gets absolutely different. For example, at the scope (A, B) the reversed C/U-plane decoupled architecture performs better. But in most situations, it possesses much poorer transmission reliability than normal C/U-plane decoupled architecture. From the trend of URF in Figure 9, it is also obvious that normal C/U-plane decoupled architecture can provide more reliable transmission than the reversed case, which exactly conforms to the consideration during the design of C/U-plane decoupled architecture that C-plane more heavily affects the transmission reliability than U-plane thereby being kept at dependable lower frequency bands. Therefore, under the proposed indicator

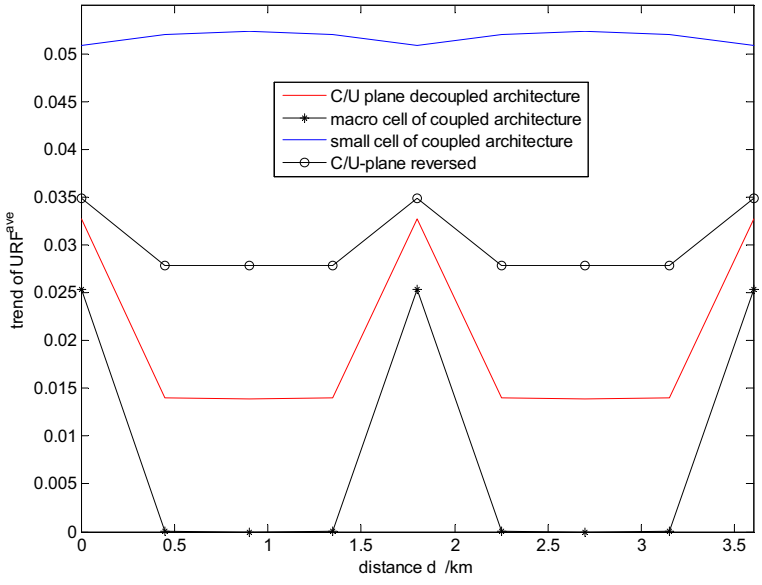

Figure 9 Trends of URF^{ave} in Figure 8.

URF, the importance of C-plane is completely reflected and it is more proper to use URF as the indicator to evaluate the transmission reliability of C/U-plane decoupled architecture.

Conclusions

For upcoming 5G wireless communication system, C/U-plane decoupled architecture is a potential way to not only expand capacity but also to prevent unnecessary control signaling overhead. In addition, we apply this architecture to future professional high-speed railway wireless communication system to fulfill the wireless access desire of train passengers during long-distance journey. However, how to properly evaluate the system transmission reliability of C/U-plane decoupled architecture becomes an urgent problem, which will impact the subsequent research direction on performance enhancement. It has been proved that the conventional outage probability cannot convey the primary design consideration of this decoupled architecture that C-plane more heavily affects the entire transmission reliability than U-plane thereby being kept at lower frequency bands. Based on this, a novel indicator URF is proposed. The theoretical analysis and numerical simulation results have confirmed that URF performs more properly in evaluating the entire system transmission reliability of C/U-plane decoupled architecture.

Competing interests

The authors declare that they have no competing interests.

Acknowledgements

The work of the authors was supported partially by the 973 Program under Grant 2012CB316100, NSFC under Grant 61032002, and the Program for Development of Science and Technology of China Railway Corporation under Grant 2013X016-A.

Received: 4 April 2014 Accepted: 27 July 2014
Published: 9 August 2014

References

1. T Nakamura, S Nagata, A Benjebbour, Y Kishiyama, T Hai, S Xiaodong, Y Ning, L Nan, Trends in small cell enhancements in LTE advanced. IEEE Commun. Mag. **51**(2), 98–105 (2013)
2. BA Bjerke, LTE-advanced and the evolution of LTE deployments. IEEE Wireless Commun. Mag. **18**(5), 4–5 (2011)
3. B Dusza, C Ide, P-B Bok, C Wietfeld, Optimized cross-layer protocol choices for LTE in high-speed vehicular environments, in *Proceedings of the 9th IEEE International Wireless Communications and Mobile Computing Conference* (Sardinia, 1–5 July 2013), pp. 1046–1051
4. W Luo, X Fang, M Cheng, Y Zhao, Efficient multiple-group multiple-antenna (MGMA) scheme for high-speed railway viaducts. IEEE Trans. Veh. Technol. **62**(6), 2558–2569 (2013)
5. L Yan, X Fang, Decoupled wireless network architecture for high-speed railway, in *Proceedings of IEEE International Workshop on High Mobility Wireless Communications,* (Shanghai, 1–3 Nov 2013), pp. 96–100
6. H Song, X Fang, L Yan, Handover scheme for 5G C/U plane split heterogeneous network in high-speed railway. IEEE Trans. Veh. Technol (2014). doi:10.1109/TVT.2014.2315231
7. X Zhu, S Chen, H Hu, X Su, Y Shi, TDD-based mobile communication solutions for high-speed railway scenarios. IEEE Wireless Commun. **20**(6), 22–19 (2013)
8. E Dahlman, S Parkvall, J Sköld, *LTE/LTE-Advanced for Mobile Broadband.* (Academic Press, Oxford, 2011)
9. X Xiuqiang, H Gaoning, Z Shunqing, C Yan, X Shugong, On functionality separation for green mobile networks: concept study over LTE. IEEE Commun. Mag. **51**(5), 82–90 (2013)
10. H Ishii, Y Kishiyama, H Takahashi, A novel architecture for LTE-B: C-plane/U-plane split and phantom cell concept, in *Proceedings of IEEE Globecom Workshops Workshop on Emerging Technologies for LTE-Advanced and Beyond-4G* (Anaheim, 3–7 Dec 2012), pp. 624–630
11. AJ Viterbi, AM Viterbi, KS Gilhousen, E Zehavi, Soft handoff extends CDMA cell coverage and increases reverse link capacity. Sel Area Commun. **12**, 1281–1288 (1994). doi:10.1109/49.329346
12. MO Hasna, MS Alouini, Outage probability of multihop transmission over Nakagami fading channels. IEEE Commun. Lett. **7**(5), 216–218 (2003)
13. J Liu, R Love, K Stewart, ME Buckley, Design and analysis of LTE physical downlink control channel, in *Proceedings of the 69th IEEE international Conference on Vehicular Technology* (Barcelona, 26–29 April 2009), pp. 1–5
14. T Rappaoort, *Wireless Communications: Principles and Practice.* (Prentice-Hall, Englewood Cliffs, 2001)
15. SS Szyszkowicz, H Yanikomeroglu, JS Thompson, On the feasibility of wireless shadowing correlation models. IEEE Trans. Veh. Technol. **59**(9), 4222–4236 (2010)
16. J Weitzen, T Lowe, Measurement of angular and distance correlation properties of log-normal shadowing at 1900 MHz and its application to design of PCS systems. IEEE Trans. Veh. Technol. **51**(2), 265–273 (2002)
17. X Yang, S Ghaheri-Niri, R Tafazolli, Downlink soft handover gain in CDMA cellular network with cross-correlated shadowing, in *Proceedings of the 54th IEEE international Conference on Vehicular Technology* (Atlantic City, 7–11 Oct 2001), pp. 276–280
18. W Luo, R Zhang, X Fang, A CoMP soft handover scheme for LTE systems in high speed railway. EURASIP J. Wireless Commun. Netw. **1**, 196 (2012). doi:10.1186/1687-1499-2012-196
19. J Salo, L Vuokko, HM El-Sallabi, P Vainikainen, An additive model as a physical basis for shadow fading. IEEE Trans. Veh. Technol. **56**(1), 13–26 (2007)
20. P Wang, P Kam, Feedback power control with bit error outage probability QoS measure on the Rayleigh fading channel. IEEE Trans. Commun. **61**(4), 1621–1631 (2013)
21. AP Dawid, Conditional independence in statistical theory. J. R. Stat. Soc. Series B (Methodological). **41**(1), 1–31 (1979)
22. J Proakis, M Salehi, *Digital Communications*. (McGraw Hill, New York, 2000)

doi:10.1186/1687-1499-2014-127
Cite this article as: Yan and Fang: **Reliability evaluation of 5G C/U-plane decoupled architecture for high-speed railway.** *EURASIP Journal on Wireless Communications and Networking* 2014 **2014**:127.